

INFLUENCE OF SOLAR ALTITUDE ON DIFFUSE FRACTION CORRELATIONS IN CYPRUS

Rogiros Tapakis¹, Silas Michaelides² and Alexandros G. Charalambides¹

¹ Cyprus University of Technology, Department of Environmental Science and Technology, Lemesos, 3603, Cyprus

² Cyprus Department of Meteorology, Nicosia, Cyprus

Summary

Irradiance levels on arbitrary sloped surfaces is a prerequisite in meteorology, solar energy applications and building sciences, especially for modelling and monitoring the performance of solar energy systems. In general, global tilted irradiance is computed as the sum of the beam component of direct irradiation on the tilted surface, diffuse tilted and reflected irradiance. These three components can be calculated by existing formulas given the Diffuse, Global Horizontal Irradiance and surface albedo. However, although for some locations both diffuse and diffuse irradiance are measured as a standard practice, in most locations, the meteorological data comprise only of measurements of Global Horizontal Irradiance.

The present research regards numerical analysis and development of empirical correlations for the computation of the hourly diffuse fraction based on the measurements of the clearness index. Solar altitude is incorporated as a parameter in the computations in order to reduce the error in the computations since it embraces the effect of the different times and dates in the computations. The extracted numerical equations are presented in terms of solar altitude in steps of 20° based on measurements recorded at the meteorological station of Athalassa, Cyprus, for a ten year period (2001-2010). The statistical analysis from the comparison (in terms of R², RMSE and MBE) showed better results for higher elevation angles, compared to lower elevation angles that correspond to early morning or late afternoon.

1. Introduction

Solar Energy is the feedstock for various applications of renewable energy sources. Thus, the necessity of using global tilted irradiance is acknowledged for the computations of the performance and monitoring of Photovoltaic (PV) Parks, meteorology, building sciences and other solar energy applications. In general, global tilted irradiance is computed as the sum of the beam component of direct irradiation on the tilted surface, diffuse tilted and reflected irradiance. These three components can be extracted using only the values of Global Horizontal (G_h) and Diffuse (G_d) Irradiances and surface albedo (Muneer, 2004).

Although for some locations both global and diffuse irradiance are measured, in most locations, meteorological data consist only of on-site measurements of G_h . Alternatively, the components of solar irradiance can be determined from satellite data; nevertheless, the high cost of satellite data and the low spatial and temporal resolution of the measurements prevent their usability.

Thus, researchers have adopted empirical correlations for the calculation of diffuse irradiance using only measurements of G_h . The first empirical model for the computation of G_d , given the G_h was proposed at 1960 by Liu and Jordan (1960). The proposed model related the clearness index (k_t) to the diffuse fraction (k_d), where k_t is defined as the ratio of G_h to extraterrestrial radiation on a horizontal surface (G_o) and k_d is defined as the ratio of G_d to G_h .

$$k_t = \frac{\text{Global Horizontal Irradiance } (G_h)}{\text{Extraterrestrial radiation on a horizontal surface } (G_o)}$$

(eq. 1)

$$k_d = \frac{\text{Diffuse Irradiance}(G_d)}{\text{Global Horizontal Irradiance}(G_h)}$$

(eq. 2)

The main objective of the current research is to include solar altitude (α) as a clustering index on the computations in order to reduce the error since it embraces the effect of the different times and dates. New empirical correlations were developed and were compared to existing Liu-Jordan type correlations.

2. Solar irradiance data - Measurements and pre-processing

The measurements were recorded at the main Solar Radiation Centre of the Meteorological Service of Cyprus, located at Athalassa, Cyprus, a semi-rural site located at the centre of the island of Cyprus (35°28'27" North, 33°23'47" East, height 165m amsl). The climate of Cyprus is intense Mediterranean Semi-arid type climate, characterized by hot dry summers and rainy, rather changeable winters. Summers and winters are separated by short autumn and spring seasons of rapid changes in weather conditions. Additionally, during spring and early summer, the atmosphere is quite hazy due to dust transferred primarily by prevailing winds from the Saharan desert (Michaelides et al., 1999).

Hourly values of horizontal (H_h), diffuse (H_d) and direct (H_b) irradiation were recorded for a ten year period, from January 2001 to December 2010. H_h and H_d were recorded using Kipp and Zonen pyranometers (model CM21), while H_b was recorded using a Kipp and Zonen pyrliometer (model CH1). The CH1 pyrliometer and the CM21 used for diffuse measurements were positioned on a Kipp & Zonen two axis solar tracker. The equipment was cleaned and aligned on a daily basis and the sensors were calibrated yearly. The long period covered by the dataset ensures that the complete range of seasonal solar angles and seasonal variations are included in the recorded data, reducing the statistical error.

In order to compute the two Liu Jordan parameters ($k_t - k_d$), several intermediate pre-processing computations were performed. At first, the irradiation measurements were converted to irradiance. Then, in order to compute the G_o , the values of the day angle, solar declination, equation of time for the sun, hour angle, zenith angle and solar altitude were calculated (Pandey and Soupir, 2012). Finally, the k_d and the k_t were computed using equations (1) and (2).

A quality control analysis of the dataset was performed in order to eliminate spurious data, data measured during night-time, possible instrumental errors, misleading ambiguous measurements, especially cosine response during the early morning or late afternoon, and enhanced values of global irradiance due to partial cloudiness (Tapakis and Charalambides, 2014). The procedure performed is proposed by the European Commission Daylight I, 1993 (Kambezidis and Adamopoulos, 1997) and data not fulfilling the proposed conditions were removed from the dataset.

The controls used are:

$$0 \leq G_d \leq 1.1G_h \quad (\text{eq. 3})$$

$$0 \leq G_h \leq 1.2G_o \quad (\text{eq. 4})$$

$$0 \leq G_d \leq 0.8G_o \quad (\text{eq. 5})$$

$$\alpha > 5^\circ \quad (\text{eq. 6})$$

$$0 \leq G_b \leq G_o \quad (\text{eq. 7})$$

Overall, out of the 87,600 recorded values of the original dataset, only 23,174 measurements fulfilled the quality control analysis and were used in the correlations; approximately 67% of the rejected values were during night-time. The resulted dataset of k_d over k_t , after the implementation of the controls is presented in Figure 1. As can be seen at Figure 1, despite the implementation of controls at the dataset a few ambiguous records are still present that do not comply with the general form of the measurements. However, these few records were not removed from the dataset, since this research intends to provide widely applicable correlations, where the manual removal of data would not be possible.

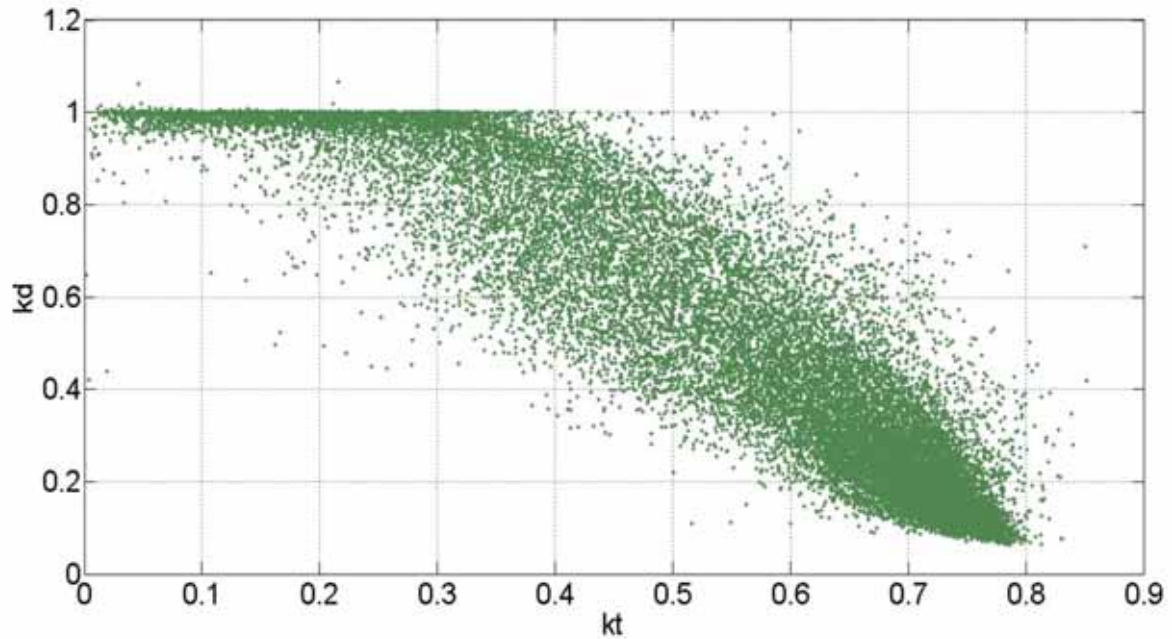


Fig. 1: k_d over k_t for the dataset after the quality control.

3. Evaluation of existing models with the controlled dataset

In general, Liu-Jordan type decomposition models are based on the variations of k_d and k_t during clear sky or cloudy conditions. During clear sky conditions (high G_h , low G_d), k_t exhibits high values and k_d exhibits low values. Conversely, during cloudy or partially cloudy conditions, G_d is increased due to the scattering of solar irradiance on water/droplet particles of the atmosphere and G_h is decreased. Thus, k_t is reduced and k_d is increased. Finally, during overcast conditions, where G_b is nearly zero and G_h approximates G_d , k_t is minimised and k_d approximates one.

The proposed Liu-Jordan type correlations quantify this effect of clouds on k_t - k_d using analytical equations, usually in a piecewise polynomial form. The original correlation proposed by Liu and Jordan (1960) was in the form:

$$k_d = 0.3840 - 0.4160k_t \quad k_t < 0.75 \quad (\text{eq. 8})$$

$$k_d = 0.16 \quad k_t > 0.75$$

The research of Liu and Jordan (1960) set the basis for the development of further decomposition models by several researchers, to fit datasets from different locations and chronological periods, which have been successful to varying degrees. Usually, the proposed correlations are simple, consisting only of a single predictor (i.e. k_t), although multinomial models were proposed, introducing additional predictors to the equations (Soares et al., 2004; Furlan et al., 2012). Since the developed models consist of empirical equations, they apply to the local dataset used for the development of the model, which is subject to the latitude of the site and the local conditions, implying that they are site specific.

23 empirical models from literature were evaluated against the dataset (after the implementation of the controls) using three common statistical indicators: Mean Bias Error (MBE), Root Mean Square Error (RMSE) and coefficient of determination (R^2). Three of the 23 models exhibited the best performance; DM (De Miguel et al., 2001) that exhibited the highest R^2 , KA (Karatassou et al., 2003) that exhibited the lowest MBE and TO (Torres et al., 2010) that exhibited the lowest RMSE. Table 1 presents the three models, the constrains of the equations and the three statistical indicators. Well worth noting is that all three models were developed using datasets from Mediterranean sites that have similar characteristics to the current site of Athalassa.

Table 1: Constrains, correlations, MBE, RMSE and R^2 of the three best fit models as applied to the dataset.

Model	Constrains	k_d	MBE (%)	RMSE (%)	R^2
DM	$kt \leq 0.21$ $0.21 < kt \leq 0.76$ $0.76 < kt$	$0.995 - 0.081k_t$ $0.724 + 2.738k_t - 8.32k_t^2 + 4.967k_t^3$ 0.18	-5.79	24.00	0.872
KA	$0 < kt \leq 0.78$ $0.78 < kt$	$0.995 - 0.05k_t - 2.4156k_t^2 + 1.4926k_t^3$ 0.2	0.31	26.51	0.862
TO	$kt \leq 0.225$ $0.225 < kt \leq 0.755$ $0.755 < kt$	$0.9943 - 0.1165k_t$ $1.4101 - 2.9918k_t + 6.4599k_t^2 - 10.329k_t^3 + 5.514k_t^4$ 0.18	-0.47	23.89	0.870

4. Dataset Clustering

In order to evaluate the influence of α on the correlations, the controlled dataset was regrouped in smaller datasets in relation to α . Four sub-datasets were formed, in steps of 20° : $0-20^\circ$, $20-40^\circ$, $40-60^\circ$ and $60-80^\circ$. The data of the first sub-group consist of measurements from morning and evening hours, when the sun is lower at the horizon. Correspondingly, the data of the fourth sub-dataset consist of measurements recorded around noon, during the summer months, when the sun is at higher α . It has to be mentioned that the first group had no records for $\alpha < 5^\circ$ due to the fourth control, while the higher α of the fourth group was 78° .

Figure 2 presents the dispersion of the datapoints on a k_d-k_t graph for each sub-dataset. A strong dependence of the k_t-k_d correlation to the elevation angle is observed, which was expected since it embraces the varying effects at different times and dates in the computations.

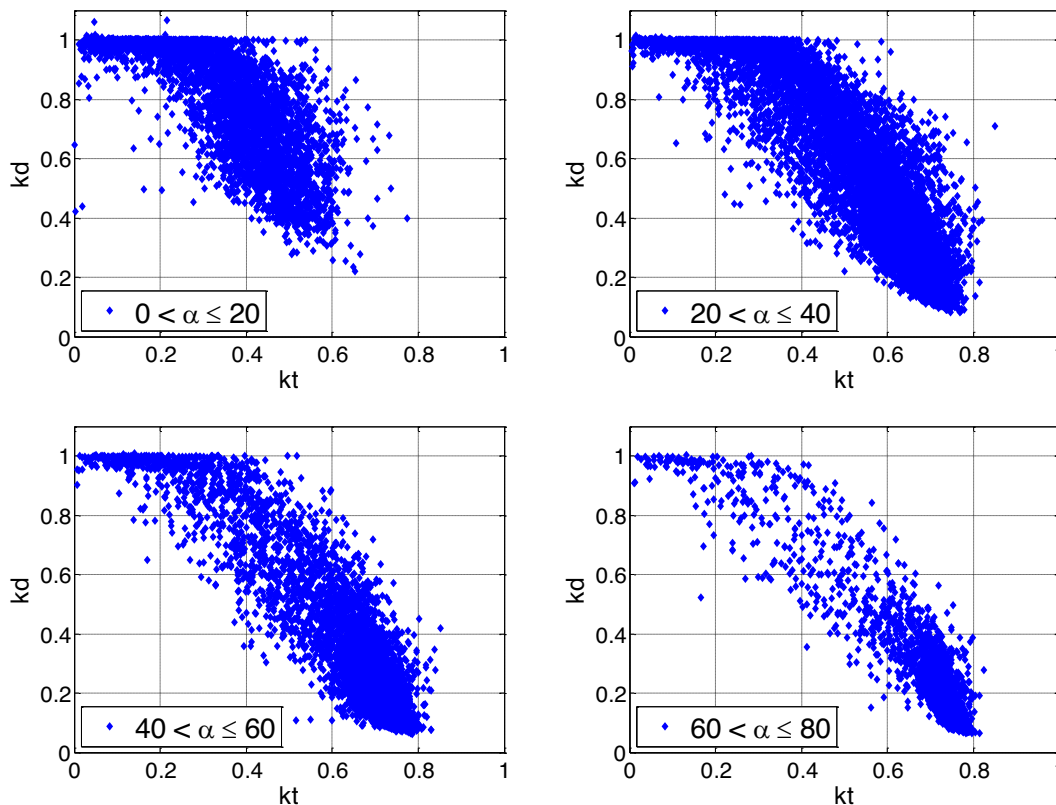


Fig. 2: Dispersion of the datapoints on a k_d-k_t graph for each sub-dataset

As expected, the progressive increase of α shifts the measurements towards higher values of k_t and lower values of k_d , whilst, since the sky is mostly cloudy free during the summer, their dispersion is decreased.

Contrary, lower solar altitude angles result in greater values of air mass, thus rendering considerable portion of global radiation as diffuse component, which can be observed from the lower k_t values and larger dispersion of the first subgroup.

Subsequently, the coefficients of the best-fit polynomial were calculated for each sub-dataset in a piecewise form, where the constrains for the individual equations consisted of the upper and lower values of α . The analytical polynomial equations for the four sub-datasets are presented in Table 2.

Table 2: The coefficients of the 5th order polynomial equations for the four sub-datasets

Solar altitude Degrees	Coefficients of 5 th order polynomial equation $k_d = p_1 + p_2 k_t + p_3 k_t^2 + p_4 k_t^3 + p_5 k_t^4 + p_6 k_t^5$					
	p ₁	p ₂	p ₃	p ₄	p ₅	p ₆
0-20	-70.91	138.99	-90.86	21.56	-1.88	1.03
20-40	28.50	-39.69	16.59	-3.98	0.36	0.98
40-60	25.21	-42.65	25.29	-8.47	1.07	0.95
60-80	36.17	-80.70	66.08	-25.05	3.26	0.86

Table 3 presents the size of the sub-datasets, and the three statistical indicators (MBE, RMSE and R^2) for each solar altitude interval and the overall accuracy for the entire dataset.

Table 3: Size of each sub-dataset, MBE, RMSE and R^2 for each solar altitude interval.

α (°)	Number of data	MBE (%)	RMSE (%)	R^2	MBE	RMSE
0-20	3974	-0.16	15.068	0.624	-0.0012	0.1177
20-40	8747	0.88	20.431	0.854	0.0047	0.1083
40-60	7023	1.92	24.624	0.897	0.0062	0.0795
60-80	3430	4.61	19.129	0.946	0.0114	0.0472
Overall	23174	1.093	22.85	0.878	0.0051	0.1071

As can be seen from the statistics of Table 3, the sub-datasets of lower solar altitude angle exhibit lower accuracy in relation to the ones of higher elevation angles, which mainly is caused due to the larger dispersion exhibited by datapoints at lower angles compared to higher ones (Figure 2). Additionally, the overall performance indicators (all three indicators) for the entire dataset are slightly improved compared to the previously presented empirical models (Table 1) which verifies the initial concept of introducing α to the computations.

An additional notable feature of Table 3 is the difference in the accuracies of the actual and percentage errors. Due to the profile of the scattering of the datapoints (Figure 2), the measurements of sub-dataset 0-20°, have lower k_t values and higher k_d values, approximating unity. Thus, percentage errors (relative RMSE and relative MBE) at Table 3 tend to exhibit unrealistic results since the mean value of the datapoints at higher α is very small, resulting to an amplification of the error. Therefore, when dealing with sub-datasets, the actual error should be used instead of the percentage error.

It has to be mentioned that the incorporation of α to the correlations does not add additional computation effort, since it is a prerequisite of the computation of G_o (Chapter 2).

5. Conclusions – Future Work

The accurate prediction of the diffuse fraction of solar radiation will enable further improvement of computational tools in meteorology and the modelling/monitoring of solar energy applications. The abundance of G_h measurements together with the limitations of (a) adequate on-site diffuse irradiance data, (b) physical modelling and (c) satellite data have led researchers to adopt empirical correlations for the calculation of diffuse irradiance using only measurements of G_h . These correlations are decomposition models based on the Liu-Jordan type correlation that relates k_t to k_d .

The present study introduces solar altitude to the correlations as a clustering parameter, in order to improve the accuracy of the models. The outcomes of this study are:

- The progressive increase of α shifts the measurements towards lower values of k_d and higher values of k_t , thus, changing the coefficients of the polynomial equations.
- Datapoints at low values of α exhibit larger dispersion compared to the datapoints at higher values of α .
- The correlations of the datasets at lower values of α exhibit lower accuracy in relation to the datasets with higher values of α .
- The low accuracy achieved for α less than 20° leads to an uncertainty in the modelling of diffuse fraction for low altitude angles.

Future work will focus on the improvement of the accuracy of the computations, by clustering the dataset in smaller sub-groups and by integrating α into the correlations using analytical equations in the form $k_t=f(k_d, \alpha)$.

Furthermore, it was observed during the analysis that the potential incorporation of additional parameters to the computations, such as the influence of time and seasons, may improve the accuracy and should be further investigated. The nonlinearity of these parameters leads to addressing the complexity of the computations using non-parametric analysis such as Artificial Neural Networks which will be assessed in future research.

6. References

- De Miguel, A., Bilbao, J., Aguiar, R., Kambezidis, H., Negro, E., 2001. Diffuse solar irradiation model evaluation in the North Mediterranean belt area. *Sol. Energy* 70, 143–53.
- Furlan, C., de Oliveira, A.P., Soares, J., Codato, G., Escobedo, J.F., 2012. The role of clouds in improving the regression model for hourly values of diffuse solar radiation. *Appl. Energ.* 92, 240–254.
- Kambezidis, H.D., Adamopoulos, A.D., 1997. In Task I CLIMED Project: Final Data Set Progress Report, NOA, Athens.
- Karatasou, S., Santamouris, M., Geros, V., 2003. Analysis of experimental data on diffuse solar radiation in Athens, Greece, for building applications. *Int. J. Sustain Energy* 23, 1-11.
- Liu, B.Y.H., Jordan, R.C., 1960. The interrelationship and characteristic distribution of direct, diffuse and total solar radiation. *Solar Energy* 4, 1–19.
- Michaelides, S., Evripidou, P., Kallos, G., 1999. Monitoring and predicting Saharan Desert dust events in the eastern Mediterranean. *Weather* 54, 359–365.
- Muneer, T., 2004. *Solar Radiation and Daylight Models*, 2nd ed. Elsevier Ltd.
- Pandey, P.K., Soupir, M.L., 2012. A new method to estimate average hourly global solar radiation on the horizontal surface. *Atmos. Res.* 114-115, 83–90.

Soares, J., Oliveira, A.P., Boznar, M.Z., Mlakar, P., Escobedo, J.F., Machado, A.J., 2004. Modeling hourly diffuse solar-radiation in the city of Sao Paulo using a neural-network technique. *Appl Energy* 79, 201-214.

Tapakis, R., Charalambides, A.G., 2014. Enhanced values of global irradiance due to the presence of clouds in Eastern Mediterranean. *Renew. Energy* 62, 459-467.

Torres, J.L., De Blas, M., García, A., de Francisco, A., 2010. Comparative study of various models in estimating hourly diffuse solar irradiance. *Renewable Energy* 35, 1325–1332.